

# Four-body structure of neutron-rich hypernucleus ${}^6_{\Lambda}\text{H}$

E. Hiyama<sup>1</sup>, S. Ohnishi<sup>1,2</sup>, M. Kamimura<sup>3</sup>, and Y. Yamamoto<sup>1</sup>

<sup>1</sup>*Nishina Center for Accelerator-Based Science,*

*Institute for Physical and Chemical Research (RIKEN), Wako 351-0198, Japan*

<sup>2</sup>*Department of Physics, Tokyo Institute of Technology, Meguro 152-8551, Japan and*

<sup>3</sup>*Department of Physics, Kyushu University, Fukuoka 812-8581, Japan*

## Abstract

The structure of heavy hyperhydrogen  ${}^6_{\Lambda}\text{H}$  is studied within the framework of a  $tnn\Lambda$  four-body cluster model. Interactions among the constituent subunits are determined so as to reproduce reasonably well the observed low-energy properties of the  $tn$ ,  $t\Lambda$  and  $tnn$  subsystems. As long as we reproduce the energy and width of  ${}^5\text{H}$  within the error bar, the ground state of  ${}^6_{\Lambda}\text{H}$  is obtained as a resonant state.

## I. INTRODUCTION

One of the research goals in hypernuclear physics is to study new dynamical features by injecting a  $\Lambda$  particle into a nucleus. For example, since there is no Pauli principle between nucleons and a  $\Lambda$  particle, the  $\Lambda$  participation gives rise to more bound states and significant contraction of nuclear cores, especially in light systems. Such a dynamical change in light hypernuclei has been studied mostly in systems composed of a stable nucleus and an attached  $\Lambda$  particle [1, 2]. In light nuclei near the neutron drip line, there have been observed interesting phenomena concerning neutron halos. A corresponding subject in hypernuclear physics is to focus on structures of neutron-rich  $\Lambda$  hypernuclei. If a  $\Lambda$  particle is added to such nuclei with weakly-bound neutrons or resonant ones, a resultant hypernucleus will become more stable against neutron decay. Thanks to this glue-like role of an attached  $\Lambda$  particle, there is a new chance to produce a hypernuclear neutron-(proton-) state, if the core nucleus has an unbound (resonant) nucleon state with an appropriate energy above the nucleon-decay threshold. Another interest is to extract information about  $\Lambda N - \Sigma N$  coupling effects in hypernuclei. It is thought that this effect might play an important role in neutron-rich  $\Lambda$  hypernuclei, because the total isospin becomes large.

For such an aim, the structure of  ${}^6_{\Lambda}\text{He}$ ,  ${}^7_{\Lambda}\text{He}$ ,  ${}^7_{\Lambda}\text{Li}$  and  ${}^7_{\Lambda}\text{Be}$  was investigated [3, 4] using an  $\alpha$  cluster model, and it was pointed out that these hypernuclei were of neutron- or proton-halo structure. One of them, the neutron-rich  $\Lambda$  hypernucleus  ${}^7_{\Lambda}\text{He}$ , was observed in the  $(e, e'K^+)$  reaction at Jlab [5], and an observed  $\Lambda$  separation energy of  $B_{\Lambda} = 5.68 \pm 0.03 \pm 0.25$  MeV was reported.

On the other hand, to produce a neutron-rich hypernucleus  ${}^{10}_{\Lambda}\text{Li}$ , the double-charge exchange  $(\pi^-, K^+)$  reaction on a  ${}^{10}\text{B}$  target was performed at KEK [6]. On the basis of the result of this experiment, Umeya and Harada [7] calculated the structure of the Li-isotope  $\Lambda$  hypernuclei within a shell-model framework, and they stressed that  $\Lambda N - \Sigma N$  coupling effects play a moderate role for the  $\Lambda$ -binding energy as the number of neutrons increases.

Recently, a FUNUDA experiment [8, 9] reported an epoch-making observation of super-heavy hydrogen- $\Lambda$  hypernucleus  ${}^6_{\Lambda}\text{H}$  as a bound state with  $B_{\Lambda} = 4.0 \pm 1.1$  MeV.  ${}^6_{\Lambda}\text{H}$  is a neutron-rich system including four neutrons and only a single proton, which goes far toward the neutron drip line. Others have previously analyzed the structure of this hypernucleus. For example, Dalitz *et al.* predicted that  ${}^6_{\Lambda}\text{H}$  was a bound state based upon shell model

arguments [10]. Akaishi *et al.* suggested that coherent  $\Lambda N - \Sigma N$  coupling is important for the  $\Lambda$  binding in  ${}^6_{\Lambda}\text{H}$  [11].

With motivation from these experimental and theoretical studies, a search (Experiment E-10) for  ${}^6_{\Lambda}\text{H}$  using the double-charge exchange ( $\pi^{-}, K^{+}$ ) reaction at J-PARC [12] has been performed, and the analysis is now in progress. Thus, it is quite timely to study the structure of  ${}^6_{\Lambda}\text{H}$  within a realistic approach.

It should be noted that the ground state of the core nucleus  ${}^5\text{H}$  was observed as a resonant state with a broad width,  $E = 1.7 \pm 0.3$  MeV ( $\Gamma = 1.9 \pm 0.4$  MeV) [13], with respect to the *tnn* three-body breakup threshold. We further note that the  $\Lambda$  separation energy,  $B_{\Lambda}$ , depends strongly on the spatial structure (size) of the core nucleus [14, 15]. Therefore, before calculating the binding energy of  ${}^6_{\Lambda}\text{H}$ , it is essential to reproduce the observed data for  ${}^5\text{H}$ . The resonant structure of  ${}^5\text{H}$  has been studied in the literature within the framework of a *tnn* three-body model; it was found that  ${}^5\text{H}$  was described well by using such a model [16, 17]. Therefore, it is reasonable to employ a *tnn* $\Lambda$  four-body model for the study of  ${}^6_{\Lambda}\text{H}$  in the present work. In order to discuss the energy and width of  ${}^5\text{H}$  on the basis of the *tnn* three-body model, we employ the complex scaling method (CSM), a powerful tool for analyzing such three-body resonance states [18–22].

All the interactions among subunits (triton, two neutrons and  $\Lambda$ ) are chosen to reproduce the appropriate low energy properties, such as binding energies and scattering phase shifts for each of the subsystems composed of two and three subunits. Using these interactions, we calculate the energy of  ${}^6_{\Lambda}\text{H}$  based on the *tnn* $\Lambda$  four-body model and discuss whether or not  ${}^6_{\Lambda}\text{H}$  exists as a bound system.

In Sect. 2, the method used in the four-body calculation for the *tnn* $\Lambda$  system is described. In Sect. 3, we explain the interactions employed. The calculated results and discussion are presented in Sect. 4. A summary is given in Sect. 5.

## II. MODEL

### A. The ${}^6_{\Lambda}\text{H}$ hypernucleus

In this work the hypernucleus  ${}^6_{\Lambda}\text{H}$  is considered as a triton cluster, a  $\Lambda$  particle, and two valence neutrons. The triton cluster is considered to be an inert core (an elementary

particle) and to have a wave function  $\Phi(t)$  with a  $(0s)^3$  shell model configuration, .

Nine sets of Jacobian coordinates for the four-body system of  ${}^6_{\Lambda}\text{H}$  are illustrated in Fig.1; additionally, we further take into account the antisymmetrization between the two neutrons.

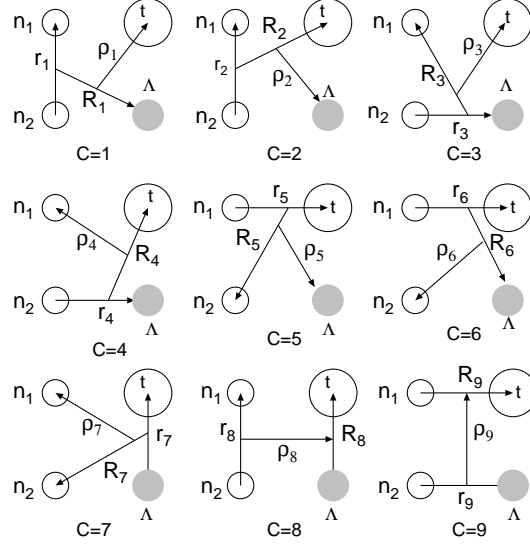


FIG. 1: Jacobi coordinates for all the rearrangement channels ( $c = 1 \sim 9$ ) of the  $tnn\Lambda$  four-body system. The two nucleons are to be antisymmetrized within each channel.

The total Hamiltonian and the Schrödinger equation are given by

$$(H - E) \Psi_{JM,TT_z}({}^6_{\Lambda}\text{Z}) = 0, \quad (1)$$

$$H = T + V_{n_1 n_2} + \sum_{i=1}^2 (V_{\Lambda n_i} + V_{t n_i}) + V_{t n_1 n_2} + V_{t \Lambda}, \quad (2)$$

where  $V_{t n_i}$  and  $V_{n_1 n_2}$  are the interactions between the triton and  $i$ -th neutron and the one between two neutrons, respectively.  $V_{t \Lambda}$  is the triton- $\Lambda$  interaction and  $V_{t n_1 n_2}$  is the triton- $nn$  three-body force. These interactions are explained in the next section. The total wave function is described as a sum of amplitudes for all the rearrangement channels shown in Fig. 1 and  $LS$  coupling scheme:

$$\begin{aligned} \Psi_{JM}({}^6_{\Lambda}\text{Z}) = & \sum_{c=1}^7 \sum_{nl, NL, \nu \lambda} \sum_{IK} \sum_{ss'S} C_{nl, NL, \nu \lambda, IK, ss'S}^{(c)} \Phi(t) \\ & \times \mathcal{A} \left\{ \left[ \left[ \left[ \phi_{nl}^{(c)}(\mathbf{r}_c) \psi_{NL}^{(c)}(\mathbf{R}_c) \right]_I \xi_{\nu \lambda}^{(c)}(\boldsymbol{\rho}_c) \right]_K \right. \right. \\ & \times \left. \left. \left[ \left[ \left[ \chi_{\frac{1}{2}}(n_1) \chi_{\frac{1}{2}}(n_2) \right]_s \chi_{\frac{1}{2}}(t) \right]_{s'} \chi_{\frac{1}{2}}(\Lambda) \right]_S \right]_{JM} \right\}, \\ & + \sum_{c=8}^9 \sum_{nl, NL, \nu \lambda} \sum_{IK} \sum_{ss'S} C_{nl, NL, \nu \lambda, IK, ss'S}^{(c)} \Phi(t) \end{aligned}$$

$$\begin{aligned}
& \times \mathcal{A} \left\{ \left[ \left[ \phi_{nl}^{(c)}(\mathbf{r}_c) \psi_{NL}^{(c)}(\mathbf{R}_c) \right]_I \xi_{\nu\lambda}^{(c)}(\boldsymbol{\rho}_c) \right]_K \right. \\
& \left. \times \left[ \left[ \chi_{\frac{1}{2}}(n_1) \chi_{\frac{1}{2}}(n_2) \right]_s \left[ \chi_{\frac{1}{2}}(t) \chi_{\frac{1}{2}}(\Lambda) \right]_{s'} \right]_{JM} \right\}. \quad (3)
\end{aligned}$$

Here, the operator  $\mathcal{A}$  stands for antisymmetrization between the two valence neutrons. In Eq. (3), the isospin coupling is omitted since  ${}^6_{\Lambda}\text{H}$  is stretched in isospin space.  $\chi_{\frac{1}{2}}(n), \chi_{\frac{1}{2}}(t), \chi_{\frac{1}{2}}(\Lambda), \eta_{\frac{1}{2}}(n)$  and  $\eta_{\frac{1}{2}}(t)$  are the spin and isospin functions of the neutron, triton and  $\Lambda$ , respectively. It is to be noted that, in Eq. (3), the way of spin and isospin coupling is the same for all the channels ( $c = 1 \sim 9$ ) simply to perform numerical calculation easily. But, we have no problem for the present calculation, since we employ the full space of the spin and isospin variables for each channel. The isospin- and spin function employed in Eq. (3) are also successfully applied to the calculation of four-nucleon bound state of  ${}^4\text{He}$ [26].

Following the Gaussian Expansion Method (GEM) [23–25, 27], we take the functional forms of  $\phi_{nlm}(\mathbf{r}), \psi_{NLM}(\mathbf{R})$  and  $\xi_{\nu\lambda\mu}^{(c)}(\boldsymbol{\rho}_c)$  as

$$\begin{aligned}
\phi_{nlm}(\mathbf{r}) &= r^l e^{-(r/r_n)^2} Y_{lm}(\hat{\mathbf{r}}), \\
\psi_{NLM}(\mathbf{R}) &= R^L e^{-(R/R_N)^2} Y_{LM}(\hat{\mathbf{R}}), \\
\xi_{\nu\lambda\mu}(\boldsymbol{\rho}) &= \rho^\lambda e^{-(\rho/\rho_\nu)^2} Y_{\lambda\mu}(\hat{\boldsymbol{\rho}}), \quad (4)
\end{aligned}$$

where the Gaussian range parameters are chosen according to geometric progressions:

$$\begin{aligned}
r_n &= r_1 a^{n-1} \quad (n = 1 - n_{\max}), \\
R_N &= R_1 A^{N-1} \quad (N = 1 - N_{\max}), \\
\rho_\nu &= \rho_1 \alpha^{\nu-1} \quad (\nu = 1 - \nu_{\max}). \quad (5)
\end{aligned}$$

The angular momentum space of  $l, L, \lambda \leq 2$  is found to be sufficient to obtain good convergence of the calculated results. Application of the GEM to the three-, four- and five-body calculations of single- and double- $\Lambda$  hypernuclei have been extensively performed and are reviewed in Refs. [27–30].

The eigenenergies  $E$  in Eq. (1) and the coefficients  $C$  in Eq. (3) are determined by diagonalizing the Hamiltonian in Eq. (2) with the use of the four-body basis functions introduced above. If the calculated lowest state is obtained below the lowest-lying  ${}^4_{\Lambda}\text{H} + n + n$  threshold, it is identified as the the bound ground state of  ${}^6_{\Lambda}\text{H}$ .

When the lowest state is not a bound state but a resonant state, we calculate the energy and width of the resonance employing the stabilization (real-scaling) method [31] that is useful in calculating narrow resonances and is tractable even in the case of four-body resonant states. (Note that we take the CSM when calculating the broad three-body resonance of  ${}^5\text{H}$  as explained below). In the stabilization method, we first diagonalize the Hamiltonian and obtain the eigenenergies in the same manner as in the bound-state calculation but changing (scaling) the Gaussian range parameters (5), for example, as  $r_n \rightarrow \alpha r_n$  ( $\alpha \sim 0.5$  to  $2$ ). The position and width of a resonance can be estimated, using Eq. (4) of Ref. [31], from the degree of the stabilization of the eigenenergy versus the scaling of the Gaussian range parameters (5). A good example of such a calculation is shown in Ref. [32] for the study of the pentaquark resonances under the scattering boundary condition.

## B. The ${}^5\text{H}$ nucleus

We assume that the  ${}^5\text{H}$  nucleus is represented by the  $tnn$  three-body system, which is a part of the entire  $tnn\Lambda$  four-body system. The sets of the Jacobi coordinates describing the  ${}^5\text{H}$  nucleus are given by the channels  $c = 2$  and  $c = 5$  in Fig. 1 but omitting the  $\Lambda$  particle and the coordinate  $\rho$ . The wave function of  ${}^5\text{H}$  is written with the use of Eq. (3) but employing the channels  $c = 2$  and  $c = 5$  only and omitting the amplitudes for the  $\Lambda$  particle. The Hamiltonian of the  $tnn$  subsystem, say  $H_{tnn}$ , is given by Eq. (2) without the terms for the  $\Lambda$  particle.

As mentioned before, the ground state of  ${}^5\text{H}$  is a resonant state which was observed at  $E_r = 1.7 \pm 0.3$  MeV with  $\Gamma = 1.9 \pm 0.4$  MeV with respect to the  $tnn$  three-body breakup threshold. In order to perform a study of such a broad, low-lying three-body resonance, we employ the CSM [18–22]. The CSM and its application to the nuclear physics problems are extensively reviewed in Ref. [33] and references therein. Very recently, various types of  $3\alpha$  resonances in  ${}^{12}\text{C}$  were studied using the CSM [34].

Using the CSM, one can directly obtain the energy  $E_r$  and the decay width  $\Gamma$  of the  $tnn$  three-body resonance by solving the eigenvalue problem for the complex scaled Schrödinger equation with a scaling angle  $\theta$ :

$$[H_{tnn}(\theta) - E(\theta)]\Psi_{tnn}(\theta) = 0, \quad (6)$$

where the boundary condition of the three-body outgoing wave is automatically satisfied for the resonance, giving  $E = E_r - i\Gamma/2$  that is, in principle, independent of  $\theta$ . The complex scaled Hamiltonian  $H_{tnn}(\theta)$  is obtained by making the radial coordinate transformation

$$r_c \rightarrow r_c e^{i\theta}, \quad R_c \rightarrow R_c e^{i\theta} \quad (c = 2 \text{ and } 5 \text{ in Fig. 1}) \quad (7)$$

in the Hamiltonian  $H_{tnn}$  of the  $tnn$  system which is introduced in Sect. IIIb.

A great advantage of the CSM is that the resonance states are described with an  $L^2$ -integrable wave function. Therefore, the resonance wave function  $\Psi_{tnn}$  can be expanded in terms of the basis functions such as Eqs. (4) and (5).

### III. INTERACTIONS

For the  $NN$  interaction  $V_{NN}$ , we take the AV8' potential [35]. For the  $\Lambda N$  interaction,  $V_{\Lambda N}$ , we employ an effective single-channel interaction simulating the basic features of the Nijmegen model NSC97f [36], where the  $\Lambda N$ - $\Sigma N$  coupling effects are renormalized into  $\Lambda N$ - $\Lambda N$  components: The potential parameters of the  $\Lambda N$  interaction are listed in Table I(a) in Ref.[4] with the three-range Gaussian potentials which are chosen to reproduce the  $\Lambda N$  scattering phase shifts calculated from the NSC97f. Then, their second-range strengths in the even states of spin-independent and spin-spin terms are adjusted so that the calculated energies of the  $0^+-1^+$  doublet states of  ${}^4_\Lambda\text{H}$  in the  $NNN\Lambda$  four-body calculation reproduce the observed energies of the states. More importantly, this  $\Lambda - N$  interaction was applied to  ${}^6_\Lambda\text{He}$  within an  $\alpha n\Lambda$  three-body model, resulting in  $\Lambda$  separation energy  $B_\Lambda = 4.21$  MeV which reproduces the observed  $B_\Lambda = 4.18 \pm 0.10$  MeV. This same  $\Lambda N$  interaction and the present  $NN$  interaction were already applied in the calculation of the binding energy of  ${}^7_\Lambda\text{He}$  within the framework of an  $\alpha\Lambda NN$  four-body model, resulting in  $B_\Lambda = 5.48$  MeV (see the result using 'even' in Fig.2 of Ref.[4].) which is consistent within the error bar with the recent data of  ${}^7_\Lambda\text{He}$  at Jlab[5]. We thus consider that the employed  $\Lambda N$  interactions in this work are reasonable.

The interaction  $V_{t\Lambda}$  is obtained by folding the  $\Lambda N$  G-matrix interaction derived from the Nijmegen model F(NF) [37] into the density of the triton cluster, its strength being adjusted so as to reproduce the experimental value of  $B_\Lambda({}^4_\Lambda\text{H})$  within the  $t\Lambda$  cluster model. Also, the spin dependence of the  $t\Lambda$  interaction is such that it reproduces the  $0^+-1^+$  doublet splitting

in  ${}^4\Lambda\text{H}$ . The potential parameters are listed in Table I(b) in Ref.[4].

As for the  $V_{tn}$ , we employ a potential proposed in Ref. [38]; it is of Gaussian shape with dependence on the angular momentum and spin of the  $tn$  system. The  $d$ - and  $f$ -wave components were taken to be the same as the  $s$  and  $p$  waves, respectively (this was noted afterwards in Ref. [39]). Additionally, we assume the same dependence for the partial waves with  $l \geq 4$  (though their effect must be negligible), and describe the resultant  $V_{tn}$  potential in the parity-dependent way:

$$\begin{aligned}
V_{tn} = \sum_{i=1}^3 \left[ \{V_{0,\text{even},i}(r) + V_{ss,\text{even},i}(r) \mathbf{S}_n \cdot \mathbf{S}_t\} \frac{1 + P_r}{2} \right. \\
+ \{V_{0,\text{odd},i}(r) + V_{ss,\text{odd},i}(r) \mathbf{S}_n \cdot \mathbf{S}_t\} \frac{1 - P_r}{2} \\
\left. + V_{\text{SO},i}(r) \boldsymbol{\ell} \cdot (\mathbf{S}_n + \mathbf{S}_t) \frac{1 - P_r}{2} \right] e^{-\mu_i r^2}, \quad (8)
\end{aligned}$$

where  $P_r$  is the space exchange (Majorana) operator.  $\mathbf{S}_n = \boldsymbol{\sigma}_n/2$  and  $\mathbf{S}_t = \boldsymbol{\sigma}_t/2$ , namely, spin operators for the neutron and triton cluster, respectively. The potential parameters of  $V_{tn}$  are listed in Table I.

TABLE I: Parameters of the triton-neutron potential  $V_{tn}$  defined by Eq. (8). The parameters are the same as in Ref. [38] except that the components for the partial waves  $l \geq 4$  are omitted there. Size parameters are in  $\text{fm}^{-2}$  and strengths are in MeV.

$i$	1	2	3
$\mu_i$	2.1	3.725	3.015
$V_{0,\text{even},i}$	205	-	-
$V_{ss,\text{even},i}$	60	-	-
$V_{0,\text{odd},i}$	-	-2.2	-13.95 @
$V_{ss,\text{odd},i}$	-	8.8	-18.6
$V_{\text{SO},i}$	-	-	4.67

However, since the observed energy of the ground state of  ${}^5\text{H}$  cannot be reproduced by using the two-body  $tn$  potential only, we introduce an effective three-body force,  $V_{tnn}$  in Eq. (2), whose definition is the same as in Ref. [17]:

$$V_{tnn} = V_{3b} e^{-(\rho_{\text{H}}/b_{3b})^2}, \quad (9)$$



where the hyperradius  $\rho_H$  is defined by

$$(m_n + m_n + m_t) \rho_H^2 = m_n r_{nn}^2 + m_t r_{tn}^2 + m_t r_{tn}^2$$

with the obvious notation. We take a range parameter of  $b_{3b} = 2.6$  fm and tune the strength parameter  $V_{3b}$  so as to reproduce the energy and width of  ${}^5\text{H}$  within the error bar of the experimental data. The details are discussed in the next section.

#### IV. RESULTS AND DISCUSSION

Before studying the structure of the hypernucleus  ${}^6_\Lambda\text{H}$ , it is essentially important to succeed in explaining the structure of the core nucleus  ${}^5\text{H}$  to which a  $\Lambda$  particle is added. We solved the CSM equation (6) and obtained the  ${}^5\text{H}$  ground state as a resonant pole with  $J = 1/2^+$ . Taking the strength of the three-body potential as  $V_{3b} = -45$  MeV, we have a resonance pole at  $E_r = 1.60$  MeV and  $\Gamma = 2.44$  MeV close to the central value of the observed energy with the error ( $E_r = 1.7 \pm 0.3$  MeV and  $\Gamma = 1.9 \pm 0.4$  MeV), which is illustrated in Fig. 2(a) for  ${}^5\text{H}$  (upper).

For  ${}^6_\Lambda\text{H}$ , due to the  $\Lambda N$  spin-spin interaction, we have  $0^+-1^+$  spin-doublet states and the  $0^+$  state is the ground state. We discuss how the energy of the  $0^+$  ground state of  ${}^6_\Lambda\text{H}$  changes with respect to the position of the  ${}^5\text{H}$  resonance as the strength  $V_{3b}$  of the  $tnn$  three-body force is increased.

As shown in Fig. 2(a), when the energy of  ${}^5\text{H}$  is close to the central value of the observed data, the ground state of  ${}^6_\Lambda\text{H}$  is obtained, with  $V_{3b} = -45$  MeV, at the total energy  $E = -0.87$  MeV ( $\Gamma = 0.23$  MeV), which is located by 1.13 MeV above the  ${}^4_\Lambda\text{H} + n + n$  threshold as a resonance. In this case, we have a  $\Lambda$  separation energy  $B_\Lambda = 2.47$  MeV with respect to  ${}^5\text{H} + \Lambda$ .

It is expected that the  $1^+$  state of  ${}^6_\Lambda\text{H}$  is located above the  $0^+$  state by about 1 MeV. This is because the two valence neutrons have spin 0 in  ${}^6_\Lambda\text{H}$ , and the  $\Lambda N$  spin-spin interaction between the two neutrons and the  $\Lambda$  particle cancels. The energy splitting of the  $0^+-1^+$  doublet states in  ${}^6_\Lambda\text{H}$  is considered to correspond to that in  ${}^4_\Lambda\text{H}$ . Therefore, in the case of (a) in Fig. 2, the  $1^+$  state is expected to lie above the  $tnn\Lambda$  four-body breakup threshold. At present, it is difficult to precisely calculate the energy and decay width of the  $1^+$  resonance using the stabilization method.

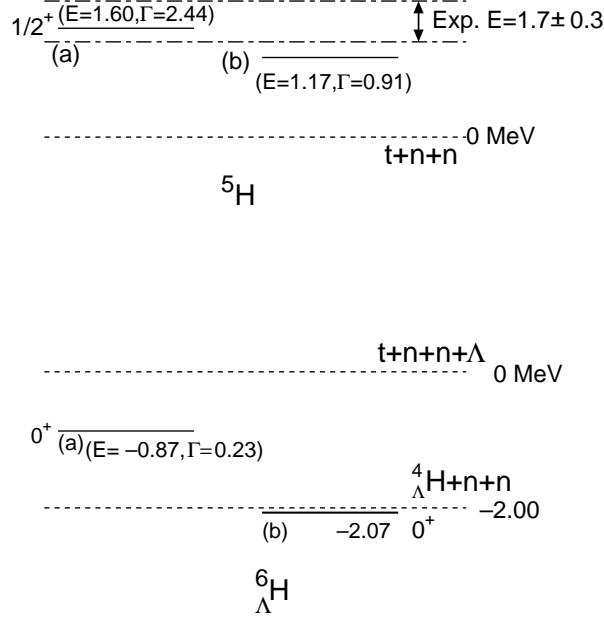


FIG. 2: Calculated energies and decay widths of  ${}^5\text{H}$  (upper) and  ${}^6_{\Lambda}\text{H}$  (lower) in the case that the  $tnn$  three-body force (9) has a strength (a)  $V_{3b} = -45$  MeV and (b)  $V_{3b} = -65$  MeV.

As the energy of  ${}^5\text{H}$  is lowered by increasing the strength of the three-body force, the energy of  ${}^6_{\Lambda}\text{H}$  becomes closer to the lowest  ${}^4_{\Lambda}\text{H} + n + n$  threshold. However, even if we adjust the calculated energy of  ${}^5\text{H}$  to the lower edge of the error band on the observed energy of  ${}^5\text{H}$ , we cannot obtain any bound state for  ${}^6_{\Lambda}\text{H}$ .

When the resonance energy of  ${}^5\text{H}$  reaches  $E_r = 1.17$  MeV with  $V_{3b} = -65$  MeV, we obtain a very weakly bound state of  ${}^6_{\Lambda}\text{H}$  at  $E = -2.07$  MeV as shown in Fig. 2(b). In this case we have  $B_{\Lambda} = 3.24$  MeV with respect to  ${}^5\text{H} + \Lambda$ , which is consistent with the FINUDA data  $B_{\Lambda} = 4.0 \pm 1.1$  MeV [8, 9] within the experimental error.

In order to demonstrate how  $B_{\Lambda}({}^6_{\Lambda}\text{H})$  depends on the energy and decay width of the core nucleus  ${}^5\text{H}$ , we consider one more case. If we have a  $tnn$  three-body force with  $V_{3b} = -73$  MeV, then we obtain a lower-lying resonance for  ${}^5\text{H}$  at  $E_r = 0.73$  MeV with  $\Gamma = 0.50$  MeV and a bound state of  ${}^6_{\Lambda}\text{H}$  at  $E = -3.02$  MeV that is 1.01 MeV below the  ${}^4_{\Lambda}\text{H} + n + n$  threshold. In this case, we have  $B_{\Lambda} = 3.75$  MeV, which is much larger than  $B_{\Lambda} = 2.47$  MeV in the case of (a) in Fig. 2. Here, we note that the energy and width of the above artificially lowered  ${}^5\text{H}$  resonance is similar to those of the ground-state resonance of the  ${}^5\text{He}$  nucleus ( $E_r = 0.80$  MeV with  $\Gamma = 0.65$  MeV), but  $B_{\Lambda}$  of  ${}^6_{\Lambda}\text{H}$  (3.75 MeV) is smaller than  $B_{\Lambda}$  of  ${}^6_{\Lambda}\text{He}$  ( $4.18 \pm 0.10$

MeV by experiment and 4.21 MeV by our calculation). This fact is reasonable. Because, two valence nucleons in  ${}^5\text{H}$  are occupied in the  $0p$  orbit. On the other hand, in  ${}^5\text{He}$  one is in the  $0p$  orbit and the other is in  $0s$  orbit. Then, this results in the weaker  $\Lambda N$  attraction (smaller  $B_\Lambda$ ) in  ${}^6_\Lambda\text{H}$  than in  ${}^6_\Lambda\text{He}$ .

As mentioned before, even if we adjust the  $tnn$  three-body force so as to match the lower limit of the error of the observed energy of  ${}^5\text{H}$ , we could have no bound state for  ${}^6_\Lambda\text{H}$ . However, by identifying  ${}^6_\Lambda\text{H}$  ground state through the observation of its two-body weak-decay  $\pi^-$  meson, the FINUDA experiment [8, 9] was able to claim that  ${}^6_\Lambda\text{H}$  is a bound system. Then, in our  $tnn\Lambda$  four-body model with no explicit  $\Lambda N$ - $\Sigma N$  coupling effect, the  ${}^5\text{H}$  resonant state should exist above the  $tnn$  three-body breakup threshold by less than 1.17 MeV.

Recently, the E-10 experiment to search  ${}^6_\Lambda\text{H}$  has been performed at J-PARC and the analysis is now in progress. If the experiment confirms the existence of this hypernucleus as a bound state, it is desirable to measure the binding energy of the core nucleus  ${}^5\text{H}$  with a precision of 100 keV.

Let us compare our results for the  $\Lambda$  separation energy  $B_\Lambda$  with those given in the literature. The shell model analysis by Dalitz [10] reported  $B_\Lambda = 4.2$  MeV. A recent shell model calculation by Millener cited in Ref. [9] gave  $B_\Lambda = 4.28 \pm 0.10$  MeV by using the three binding energies of  ${}^5_\Lambda\text{He}$  ( $B_\Lambda = 3.12 \pm 0.02$  MeV),  ${}^7_\Lambda\text{He}$  ( $B_\Lambda = 5.36 \pm 0.09$  MeV), and  ${}^4_\Lambda\text{H}$  ( $B_\Lambda = 2.04 \pm 0.04$  MeV). The results for  $B_\Lambda$  of  ${}^6_\Lambda\text{H}$  from those shell model calculations are similar to the observed data of  ${}^6_\Lambda\text{H}$ . Akaishi *et al* [11], however, obtained  $B_\Lambda = 5.8$  MeV, which is by  $\sim 1.5$  MeV larger than the above two shell-model results. Each of these three results for  $B_\Lambda$  are much larger than the  $B_\Lambda$  from the present calculation. The difference comes from whether or not the core nucleus  ${}^5\text{H}$  is taken into account explicitly in the calculations as a broad three-body resonant state.

Here, it should be reiterated that  $\Lambda N - \Sigma N$  coupling is not explicitly treated in our model. Since the total isospin of  ${}^5\text{H}$  is  $3/2$ , it is likely that the coupling plays an important role, especially, working as an effective  $\Lambda NN$  three-body force in the binding energies of  ${}^6_\Lambda\text{H}$ . So far, some authors have investigated the role of the  $\Lambda N - \Sigma N$  coupling in the binding energies of  ${}^3_\Lambda\text{H}$ ,  ${}^4_\Lambda\text{H}$  and  ${}^4_\Lambda\text{He}$  [40–47]. For example, in Ref. [46], four-body calculations for  ${}^4_\Lambda\text{H}$  and  ${}^4_\Lambda\text{He}$  were performed taking account of the  $\Lambda N$ - $\Sigma N$  coupling explicitly, and it was found that the effective  $\Lambda NN$  three-body force contributes about 0.6 MeV to the binding energy of the  $0^+$  ground state in the case of the NSC97f  $YN$  interaction. As far as the

neutron-rich hypernucleus  ${}^6_{\Lambda}\text{H}$  is concerned, Akaishi *et al.* [11] argued that  $\Lambda N$ - $\Sigma N$  coupling gave a large contribution to its binding energy. On the other hand, a recent shell model calculation by Millener cited in Ref. [48] found that the  $\Lambda N - \Sigma N$  contribution is small in  ${}^6_{\Lambda}\text{H}$ . Thus, the determination of the size of the effect in the binding energy of  ${}^6_{\Lambda}\text{H}$  is still unsettled. To answer the question, it is necessary to perform a coupled-channel calculation taking into account the  $tnn\Lambda$  and  $t({}^3\text{He})NN\Sigma$  channels. This is one of our future subjects. The new data from the search for  ${}^6_{\Lambda}\text{H}$  in Experiment E-10 at J-PARC will provide us with useful information about  $\Lambda N$ - $\Sigma N$  coupling.

Finally, it is interesting to examine the spatial structure of the ground state of  ${}^6_{\Lambda}\text{H}$  when the state becomes bound as in Fig. 2(b). Using our wave function of this state, we calculated the single-particle density distributions of the constituent particles and plotted them in Fig. 3; the dotted curve denotes the density of the  $0s$  nucleon in the triton, the dashed curve is for the  $\Lambda$  particle and the solid line for one of the two valence neutrons. The  $\Lambda$  particle is bound to the triton cluster mostly in the  $0s_{\Lambda}$  orbit that is much shallower than the  $0s$  orbit of the nucleon in the triton, whereas the valence nucleons are very loosely coupled to the triton. Thus, we see, as should be anticipated, that there are three layers in the matter distribution of the hypernucleus  ${}^6_{\Lambda}\text{H}$ , namely, the nucleons in the well bound triton core, the loosely bound  $\Lambda$  skin in the  ${}^4_{\Lambda}\text{H}$  subsystem, and the two-neutron halo that is unbound in  ${}^5\text{H}$ .

## V. SUMMARY

We have studied the structure of the neutron rich hypernucleus  ${}^6_{\Lambda}\text{H}$  within the framework of a  $tnn\Lambda$  four-body model. For this study of  ${}^6_{\Lambda}\text{H}$ , it is essentially important to reproduce the property of the ground state of the core nucleus  ${}^5\text{H}$  which is a low-lying, broad three-body resonance at  $E_r = 1.7 \pm 0.3$  MeV ( $\Gamma = 1.9 \pm 0.4$  MeV) with respect to the  $t+n+n$  threshold. We note that the  $\Lambda$  separation energy,  $B_{\Lambda}$ , depends strongly on the spatial size of the core nucleus [14, 15]. We thus utilize a  $tnn$  three-body model for the  ${}^5\text{H}$  nucleus and treat both  ${}^5\text{H}$  and  ${}^6_{\Lambda}\text{H}$  consistently.

In the present  $tnn\Lambda$  model, all the two-body interactions among subunits (triton, two neutrons and  $\Lambda$ ) are chosen to reproduce the low energy properties, such as binding energies and scattering phase shifts of each of the subsystems composed of two and three subunits.

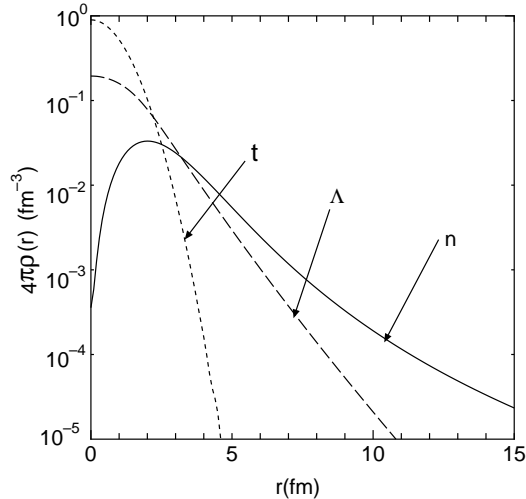


FIG. 3: Single-particle densities of the  $0s$  nucleons comprising the triton (dotted curve), the  $\Lambda$  particle (dashed curve) and one of the valence neutrons (solid curve) in the ground state of the hypernucleus  ${}^6_{\Lambda}\text{H}$  when the state becomes a bound state shown in Fig. 2(b). The radius  $r$  is measured from the c.m. of the triton.

The  $NN$  interaction is given by the AV8' potential [35]. We employ a  $\Lambda N$  effective potential that simulates  $\Lambda N$  scattering phase shifts of the NSC97f interaction [36] and is slightly tuned to reproduce the observed energies of the spin-doublet  $0^+-1^+$  states of  ${}^4_{\Lambda}\text{H}$ . The  $\Lambda N - \Sigma N$  coupling is renormalized into the  $\Lambda N$  potential. But, we note that there remains an effective  $\Lambda NN$  three-body force that is not renormalizable into the effective  $\Lambda N$  potential. The employed  $\Lambda N$  interaction reproduces the observed binding energies of  ${}^6_{\Lambda}\text{He}$  and  ${}^7_{\Lambda}\text{He}$ [4] within the framework of  $\alpha\Lambda N$  and  $\alpha\Lambda NN$  three- and four-body models, respectively.

The  $tn$  potential is taken from Ref. [38, 39]. We found that the observed resonance energy of  ${}^5\text{H}$  cannot be reproduced with the two-body  $NN$  and  $tn$  interactions only, and therefore we introduced a phenomenological, attractive  $tnn$  three-body force. When the  $tnn$  force is tuned to reproduce the central value of the observed  ${}^5\text{H}$  resonance energy, we obtain  $E_r = 1.60$  MeV ( $\Gamma = 2.44$  MeV) and, at the same time, we have the  ${}^6_{\Lambda}\text{H}$  ground state as a resonance at  $E = -0.87$  MeV ( $\Gamma = 0.23$  MeV) with respect to the  $t + n + n + \Lambda$  threshold; it is located 1.13 MeV above the lowest  ${}^4_{\Lambda}\text{H} + n + n$  threshold (Fig. 2(a)). In this case, we have  $B_{\Lambda} = 2.47$  MeV. Even if the  $tnn$  three-body force were adjusted to reproduce the lower band ( $E_r = 1.4$  MeV) based on the error of the observed  ${}^5\text{H}$  resonance energy, we could not

obtain any bound state for  ${}^6_{\Lambda}\text{H}$  below the  ${}^4_{\Lambda}\text{H} + n + n$  threshold.

We were able to generate a shallow bound state of  ${}^6_{\Lambda}\text{H}$  at  $E = -2.07$  MeV (by 0.07 MeV below the  ${}^4_{\Lambda}\text{H} + n + n$  threshold) if the  $tnn$  three-body force is tuned to have the  ${}^5\text{H}$  resonance at  $E = 1.17$  MeV ( $\Gamma = 0.91$  MeV) which is, however, 0.23 MeV below the quoted lower band of the error on the observed energy (Fig. 2(b)). In this case, we have  $B_{\Lambda} = 3.24$  MeV, which is consistent with the FINUDA data ( $B_{\Lambda} = 4.0 \pm 1.1$  MeV) within the error.

In order to study the structure of  ${}^6_{\Lambda}\text{H}$  more fully, we anticipate having a more precise value for the resonance energy of  ${}^5\text{H}$  (100 keV accuracy). It should be noted that we did not explicitly include  $\Lambda N - \Sigma N$  coupling in the present work. If, in the analysis of the E-10 experiment at J-PARC, now in progress,  ${}^6_{\Lambda}\text{H}$  is confirmed to exist as a bound state, we could obtain useful information about  $\Lambda N - \Sigma N$  coupling. To study the effect of such coupling, it is essential to perform a coupled  $tnn\Lambda + t({}^3\text{He})NN\Sigma$  four-body calculation. This calculation will be one of our future endeavors.

### Acknowledgments

The authors thank Professors T. Bressani, S. Marcello, E. Botta, A. Feliciello, A. Gal and B.F. Gibson for informative discussions. Also the authors thank Dr. S. Gojuki for support of numerical calculation. The numerical calculations were performed on the HITACHI SR16000 at KEK and YITP. This work was supported by Grants-in-Aid for Scientific Research from Monbukagakusho of Japan (No.23224006).

- 
- [1] T. Motoba, H. Bandō, and K. Ikeda, Prog. Theor. Phys. **70**, 189 (1983); H. Bandō, K. Ikeda, T. Motoba, Y. Yamamoto, and T. Yamada, Prog. Theor. Phys. Suppl. No.81, 42(1985).
  - [2] H. Bandō, T. Motoba, and J. Žofka, Int. J. Mod. Phys. A **5**, 4021 (1990).
  - [3] E. Hiyama, M. Kamimura, T. Motoba, T. Yamada, and Y. Yamamoto, Phys. Rev. **C53**, 2075 (1996).
  - [4] E. Hiyama, Y. Yamamoto, T. Motoba and M. Kamimura, Phys. Rev. **C80**, 054321 (2009).
  - [5] S. N. Nakamura *et al.*, Phys. Rev. Lett. **110**, 012502 (2013).
  - [6] P.K. Saha *et al.*, Phys. Rev. Lett. **94**, 052502 (2005).
  - [7] A. Umeya and T. Harada, Phys. Rev. **C83**, 034310 (2011).

- [8] M. Angello *et al.*, Phys. Rev. Lett. **108**, 042501 (2012).
- [9] M. Angello *et al.*, Nucl. Phys. A **881**, 269 (2012).
- [10] R. H. Dalitz and R. Levi-Setti, Nuovo Cimento **30**, 489 (1963).
- [11] Y. Akaishi and T. Yamazaki, in *Physics and Detectors for DAΦNe*, Frascati Physics Series Vol. 16 (SIS INFN-LNF, Rome, 1999), p.59; S. Shinmura, K. S. Myint, T. Harada, and Y. Akaishi, J. Phys. G **28**, L1 (2002).
- [12] A. Sakaguchi *et al.* (2006), J-PARC proposal No.E10.
- [13] A. A. Korshennikov *et al.*, Phys. Rev. Lett. **87**, 092501 (2001).
- [14] E. Hiyama, M. Kamimura, T. Motoba, T. Yamada, and Y. Yamamoto, Phys. Rev. Lett. **85**, 270 (2000).
- [15] E. Hiyama and Y. Yamamoto, Prog. Theor. Phys. **128**, 105 (2012).
- [16] N. B. Schul'gina, B. V. Danilin, L. V. Grigorenko, M. V. Zhukov and J. M. Bang, Phys. Rev. C **62**, 014312 (2000).
- [17] R. de Diego, E. Garrido, D. V. Fedorov, and A. S. Jensen, Nucl. Phys. A **786**, 71 (2007).
- [18] J. Aguilar, and J.M. Combes, Commun. Math. Phys. **22**, 269 (1971).
- [19] E. Balslev, and J.M. Combes, Commun. Math. Phys. **22**, 280 (1971).
- [20] B. Simon, Commun. Math. Phys. **27**, 1 (1972).
- [21] Y. K. Ho, Phys. Rep. **99**, 1 (1983).
- [22] N. Moiseyev, Phys. Rep. **302**, 211 (1998).
- [23] M. Kamimura, Phys. Rev. A **38**, 621 (1988).
- [24] H. Kameyama, M. Kamimura and Y. Fukushima, Phys. Rev. C **40**, 974 (1989).
- [25] E. Hiyama, Y. Kino, and M. Kamimura, Prog. Part. Nucl. Phys. **51**, 223 (2003).
- [26] H. Kamada *et al.*, Phys. Rev. C **64**, 044001 (2001).
- [27] E. Hiyama, Prog. Theor. Exp. Phys. (2012) 01A204.
- [28] E. Hiyama and T. Yamada, Prog. Part. Nucl. Phys. **63**, 339 (2009).
- [29] E. Hiyama, M. Kamimura, Y. Yamamoto, T. Motoba, and Th.A. Rijken, Prog. Theor. Phys. Supplement **185**, 106 (2010); **185**, 152 (2010).
- [30] E. Hiyama, Few-Body Systems **53**, 189 (2012).
- [31] J. Simons, J. Chem. Phys. **75**, 2465 (1981).
- [32] E. Hiyama, M. Kamimura, A. Hosaka, H. Toki and M. Yahiro, Phys. Lett.B **633**, 237 (2006).
- [33] S. Aoyama, T. Myo, K. Kato, and K. Ikeda, Prog. Theor. Phys. **116**, 1 (2006).

- [34] S.-I. Ohtsubo, Y. Fukushima, M. Kamimura, and E. Hiyama, arXiv:1302.4256 [nucl-th].
- [35] B.S. Pudliner, V. R. Pandharipande, J. Carlson, S. C. Pieper, and R. B. Wiringa, Phys. Rev. **C56**, 1720 (1997).
- [36] Th. A. Rijken, V. G. J. Stoks and Y. Yamamoto, Phys. Rev. **C59**,21 (1999); V. G. J. Stoks and Th. A. Rijken, *ibid.* **C59**, 3009 (1999).
- [37] M. M. Nagels, T. A. Rijken, and J. J. deSwart, Phys. Rev. **D15**, 2547 (1997): **20**, 1633 (1979).
- [38] N. B. Schul'gina, B. V. Danilin, V. D. Efros, J. S. Baagen, M. V. Zhukov, Nucl. Phys. A **597**, 197 (1996).
- [39] L.V. Grigorenko, B.V. Danilin, V.D. Efros, N.B. Schul'gina, and M.V. Zhukov, Phys. Rev. C **57**, R2099 (1998).
- [40] R. H. Dalitz and B. W. Downs, Phys. Rev. **111**, 967 (1958).
- [41] B. F. Gibson, A. Goldberg, and M. S. Weiss, Phys. Rev. **C6**, 741 (1972).
- [42] B. F. Gibson and D. R. Lehman, Phys. Rev. **C37**, 679 (1988).
- [43] K. Miyagawa and W. Glöckle, Phys. Rev. **C48** , 2576(1993); K. Miyagawa, H. Kamada, W.Glöckle, H. Yamamura, T. Mart, and C. Bennhold, Few-Body Syst., Suppl. **12**, 234 (2000).
- [44] J. Carlson, in LAMPF Workshop on  $(\pi, K)$  Physics, edited by B. F. Gibson, W. R. Gibbs, and M. B. Johnson, AIP Conf. Proc. No. 224, p.198 (AIP, New York, 1999).
- [45] Y. Akaishi, T. Harada, S. Shinmura, and Khin Swe Myint, Phys. Rev. Lett. **84**, 3539 (2000).
- [46] E. Hiyama, M. Kamimura, T. Motoba, T. Yamada, and Y. Yamamoto, Phys. Rev. **C65**, 011301(R) (2001).
- [47] H. Nemura, Y. Akaishi, and Y. Suzuki, Phys. Rev. Lett. **89**, 142504 (2002).
- [48] D. J. Millener, Nucl. Phys. A**881** 298 (2012).